

# Exponential Diffusion Tensors for efficient higher-order DT-MRI computations

A. Barmpoutis<sup>1</sup>, B. C. Vemuri<sup>1</sup>, and T. M. Shepherd<sup>2</sup>

<sup>1</sup>Computer and Information Sciences and Engineering, University of Florida, Gainesville, Florida, United States, <sup>2</sup>Department of Neuroscience, University of Florida

**Abstract** - In DT-MRI processing a 2nd order tensor has been commonly used to approximate the diffusivity profile at each lattice point of the 2D or 3D image. These tensors are symmetric positive definite matrices and the appropriate handling of this property increases significantly the complexity and the execution times of the algorithms. In this paper we present a novel parameterization of the diffusivity profile. Using this parameterization the positive definite property of the diffusivity is guaranteed without the need of any further computation. This parameterization can also be used for higher order approximations; we present 4, 6 and 8th order tensor approximations. Furthermore, we present an efficient framework for computing distances and geodesics on the space of the coefficients of our proposed diffusivity function. We validate our method using real diffusion weighted MR data from excised, perfusion-fixed rat optic chiasm (fig. 1).

**Motivation** – The standard diffusivity function  $d(\mathbf{g})=\mathbf{gDg}^T$  gives a 2nd order approximation of the true diffusivity. Higher order approximations can be obtained by generalizing the diffusivity function  $\sum g_1^i g_2^j g_3^k D_{i,j,k}$ . However there is no proposed framework able to handle computations of higher order tensors preserving the positive definite property.

**Proposed Framework** – In our work we employ the diffusivity function  $d(\mathbf{g})=\exp(\mathbf{gEg}^T)$ , where  $\mathbf{g}$  is a unit vector. This function is positive definite for any symmetric matrix  $\mathbf{E}$ . Similarly in the higher order case we employ the function  $\exp(\sum g_1^i g_2^j g_3^k E_{i,j,k})$ . In order to make computations in the space of the proposed diffusivity functions we use the L-2 distance between  $d_1(\mathbf{g})=\exp(\mathbf{gE}_1\mathbf{g}^T)$  and  $d_2(\mathbf{g})=\exp(\mathbf{gE}_2\mathbf{g}^T)$  given by  $dist^2(\mathbf{E}_1, \mathbf{E}_2) = \int (\log(d_1(\mathbf{g})) - \log(d_2(\mathbf{g})))^2$ . We computed analytically the integral over all unit vectors  $\mathbf{g}$  for the case of 2, 4, 6 and 8th order approximations and it can be expressed as a sum of powers of the elements of  $\mathbf{E}_1$  and  $\mathbf{E}_2$  which can be implemented very efficiently. Using this distance measure we prove that the mean element can be computed as Euclidean mean and geodesics can be computed as in the Euclidean space. The coefficients  $\mathbf{E}$  can be estimated from diffusion weighted images by following a functional minimization method as in the case of standard diffusivity function. Processing of the estimated field of coefficients  $\mathbf{E}$  can be done efficiently by using standard vector field processing methods (fig. 2,3). Finally, we can compute the distance from the closest isotropic case which has similar behavior to the standard fractional anisotropy map (fig. 4).

**Experimental Results** – We estimated 4, 6 & 8th order approximations from a dataset acquired from a rat optic-chiasm (fig. 1) and then we computed the mean and the principal components (fig. 2). We present also distance map from the isotropy (fig. 4) and a comparison of our proposed function with the standard diffusivity function (fig. 5). For the case of higher order approximations we compute and plot the probability profiles instead of the diffusivity profiles. Figures are explained with more details in their captions.

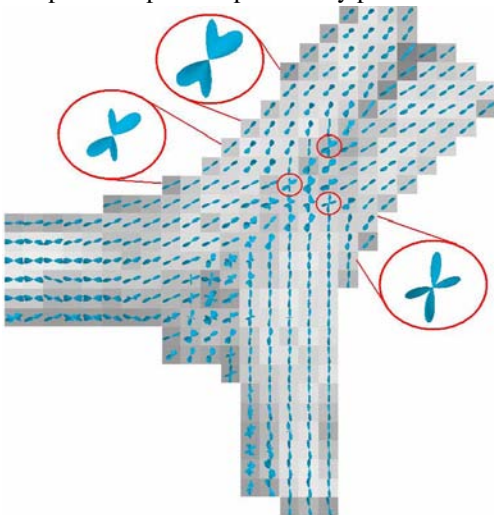


**Figure 1:** Plot of the estimated probability profiles using 4th order approximations of a dataset acquired from excised, perfusion-fixed rat optic chiasm. The probability profiles demonstrate the distinct fiber orientations in the central region of the optic chiasm where myelinated axons from the two optic nerves cross one another to reach their respective contralateral optic tracts. These orientation maps are consistent with other published works on this anatomical region of the rat nervous system.

**MEAN      6 OF THE PRINCIPAL COMPONENTS**



**Figure 2:** Example of statistical analysis of the data from fig.1 using our framework. Using Euclidean mean and the standard PCA we can compute the mean and the principal components of the data. Here probability profiles plotted.

**INTERPOLATION**



**Figure 3:** Interpolation example using our method. Given the first and third profile we compute the interpolant in the center.

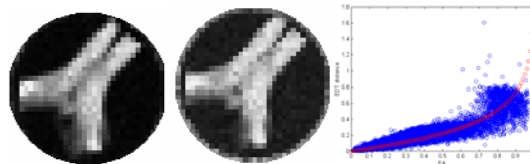


**Figure 4:** Comparison between the FA map (left) and the distance from the closest isotropic case (center) for the same dataset. On the right we plot the distance from the isotropy as a function of the FA using the same dataset.

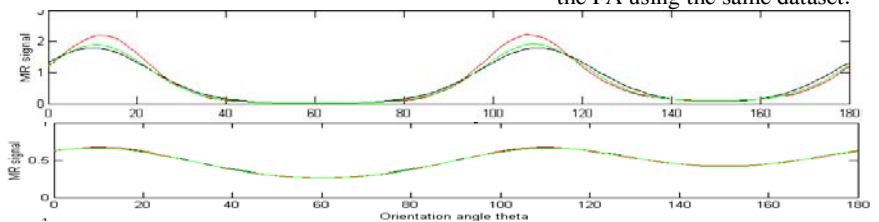


**Figure 5:** Comparison of the standard diffusivity function (red) and our proposed diffusivity function (green). Both functions approximate two given signals (black). In the upper plot the signal is sharper than the one in the lower plot. The proposed diffusivity approximates better the signal in both cases compared to the standard diffusivity function which fails in approximating the sharper signal.